

This is a non-peer reviewed pre-print submitted to EarthArXiv.

Subsequent peer-reviewed versions of this manuscript may have slightly different content.

The authors welcome feedback.

Please contact Sandy H.S. Herho ([herho@umd.edu](mailto:herho@umd.edu)) regarding this manuscript's content.

# 1 Does ENSO significantly affect rice 2 production in Indonesia? A preliminary 3 study using computational time-series 4 approach

5 Sandy H. S. Herho<sup>1</sup>, Ferio Brahmana<sup>2</sup>, Katarina E. P. Herho<sup>3</sup>, and Dasapta  
6 E. Irawan<sup>4</sup>

7 <sup>1</sup>Department of Geology, College of Computer, Mathematical, and Natural Sciences,  
8 University of Maryland, College Park, MD, USA 20742

9 <sup>2</sup>Pacmann Academy, Algoritma Cerdas Indonesia Inc., South Jakarta, Special Capital  
10 Region of Jakarta, Indonesia 12540

11 <sup>3</sup>Geological Engineering Study Program, Faculty of Earth Technology and Energy,  
12 Trisakti University, West Jakarta, Special Capital Region of Jakarta, Indonesia 10110

13 <sup>4</sup>Applied Geology Research Group, Faculty of Earth Sciences and Technology,  
14 Bandung Institute of Technology (ITB), West Java, Indonesia 40132

15 Corresponding author:

16 Sandy H. S. Herho<sup>1</sup>

17 Email address: herho@umd.edu

## 18 ABSTRACT

19 ENSO is a phenomenon that is suspected to influence rice production in Indonesia. In this study, we  
20 try to find a direct correlation between ENSO and rice production in this region by using various latest  
21 computational time series methods, such as Dynamic Time Warping, Wavelet Coherence, and Bayesian  
22 Structural Time Series to quantify the statistical relationship between the Multivariate ENSO Index on  
23 annual rice production in 1961 - 2019. We did not find a direct correlation between these two variables,  
24 which may be due to the local influence of ENSO on different rice production areas in Indonesia.

## 25 1 INTRODUCTION

26 Indonesia is the world's third biggest rice producer in 2019 (Wright, 2020). The rice crop, which is also  
27 known as paddy, itself is one of the crops heavily influenced by rainfall (Nguyen, 2005). For this reason, it  
28 is very important for Indonesia to know the effect of climate on rice production. This article hope to find  
29 relationship between Multivariate ENSO Index (MEI) (Wolter and Timlin, 1998), a phenomena which  
30 will influenced rainfall periodically, and rice production. With a simple model, due to the needs of its  
31 simplicity so that it can be digest easily by researchers from the various field of studies-, we try to find if  
32 there is any correlation between these two variables. Aside from using simple model, consistent with our  
33 accessibility information, we also try to execute our study by using open-source software.

34 One of the most similar study by Naylor et al. (2001), which also inspires this paper, had found that  
35 ENSO has strong connections with Java's rice production. However, this study is using year-to-year  
36 change of rainfall and 4-month sea surface temperature anomalies (SSTA) which represent ENSO's effects  
37 and try to fit it with year-to-year rice production in Java. This study did not use MEI directly while the  
38 index is the ENSO's intensity representation. There are also another recent studies had try to build and  
39 find any correlation between ENSO phenomena and rice production specifically in Asia and South East  
40 Asia (SEA) where rice is one of the primary food.

41 The first one (Roberts et al., 2009) is tackling the same issue in Philippines with same method as in  
42 Java's study with addition of ecosystems and fitting target variability. The study also find association  
43 between rainfall, SSTA, and rice production, harvested area, also the yield in one of the Philippines'

44 island, Luzon. There is also one other study conducted in China which adopts this method (using SSTA  
 45 rather than MEI) for their work (Deng et al., 2010) which do not find any strong correlation between  
 46 ENSO event and rice production even when the SSTA has a strong correlation with rainfall.

47 Then, there is one study by Ismail and Chan (2019) that we could find which are using MEI as one of  
 48 other variables in their pooled mean group estimation to find the correlation between the ENSO event and  
 49 rice production in SEA. However, the MEI is used together with irrigation area, fertilizer consumption,  
 50 and harvested area. We believe those other variables are arising more complexities which will affect the  
 51 difficulties of the result interpretation. This study too find that there is an association between ENSO  
 52 intensity and rice production in SEA.

53 With all of those precedents, as stated before, this study will try to differentiate by building a simpler  
 54 model that investigate the correlation between MEI Index and rice production only. As for the method, to  
 55 test the robustness of our result, we are using three kind of correlation analysis which consist of Dynamic  
 56 Time Wrapping (DTW), Wavelet Coherence (WTC), and Bayesian Structural Time Series (BSTS). After  
 57 estimating their correlation, we also provide further discussion about the results.

## 58 2 COMPUTATIONAL ANALYSIS

59 The first step we take is to calculate annual rice yield index, which is a standardized comparison of total  
 60 rice production  $P$  (in tonnes) with the area of production  $A$  (in hectare) based on FAO data (FAO, 1997)  
 61 (equation (1)).

$$I = \frac{P}{A} \quad (1)$$

We define the annual standardized rice yield index (ASRYI)  $\hat{I}$  through equation (2) below,

$$\hat{I}_i = \frac{I_i - \bar{I}}{SD} \quad (2)$$

62 , where  $\bar{I}$  and  $SD$  are respectively the mean and standard deviation of the data defined according to  
 63 equation (3) as follows,

$$\bar{I} = \frac{1}{N} \sum_{i=1}^N I_i \quad (3)$$

$$SD = \sqrt{\frac{1}{N-1} \sum_{i=1}^N (I_i - \bar{I})^2}$$

64 , where  $N$  is the number of data points, i.e. 59. The results of the time-series reconstruction of this  
 65 index can be seen in Figure 1 below,

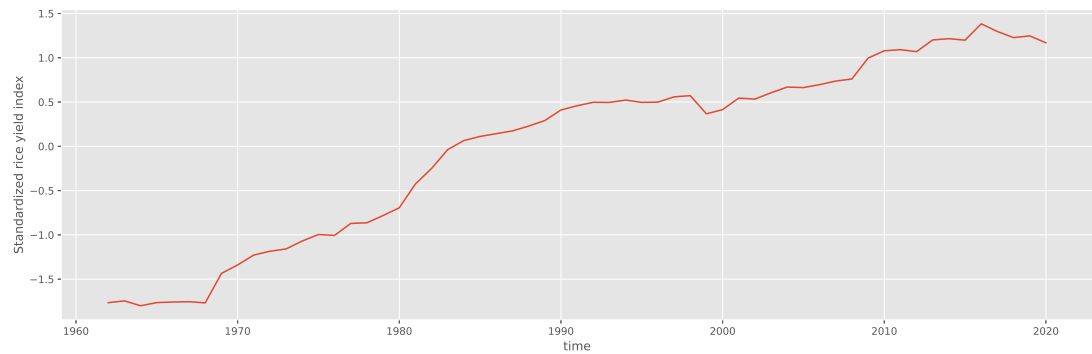


**Figure 1.** ASRYI in Indonesia from 1961 to 2019. In general, there was a rapid increase from 1961 to 2019, which is in accordance with a study conducted by Panuju et al. (2013).

66 In order to measure the similarity between ASRYI  $x$  and annual average of MEI  $y$  signals, we use a  
 67 dynamic time warping (DTW) algorithm (Sakoe and Chiba, 1978). DTW is an algorithm that is commonly  
 68 used to determine the optimal distance between two sequential data pieces to determine the similarity  
 69 between the two time-series patterns (Berndt and Clifford, 1994). Identification of the similarity of the  
 70 sequential data is done by comparing the optimal computation time to find the shortest distance between  
 71 the two sequences.

72 The first step is to input both time-series  $x_{1:N}$  and  $y_{1:N}$  data, which have the same sequence length, so  
 73 that we can form a cost matrix  $D \in \mathbb{R}^{(N+1) \times (N+1)}$ . Then, we initialize the cost matrix values as follows,  
 74  $D_{0,0} = 0$ ; for every  $i^{\text{th}}$  up to  $N^{\text{th}}$  row,  $D_{i,0} = \infty$ ; and for every  $j^{\text{th}}$  up to  $N^{\text{th}}$  column,  $D_{i,0} = \infty$ . Then, for  
 75 each row component  $i = 1$  and column  $j = 1$  to the  $N^{\text{th}}$  row and column, the components of the cost  
 76 matrix are calculated using the following equation,

$$D_{i,j} = d(x_i, y_j) + \min \begin{cases} D_{i-1,j-1} & \text{(match)} \\ D_{i-1,j} & \text{(insertion)} \\ D_{i,j-1} & \text{(deletion)} \end{cases} \quad (4)$$

77 in this study we use Euclidean distance to measure  $d(x_i, y_j)$ . We need to trace back the components  
 78 of the cost matrix from  $D_{N,N}$  to  $D_{0,0}$  to get the alignment of these two sequences. To automate this  
 79 computation, we use an implementation of the FastDTW algorithm (Salvador and Chan, 2004) which is  
 80 implemented in the Python computing environment via the **dtw-python** library (Giorgino, 2009). The 2D  
 81 cost matrix representation is shown in Figure 2.

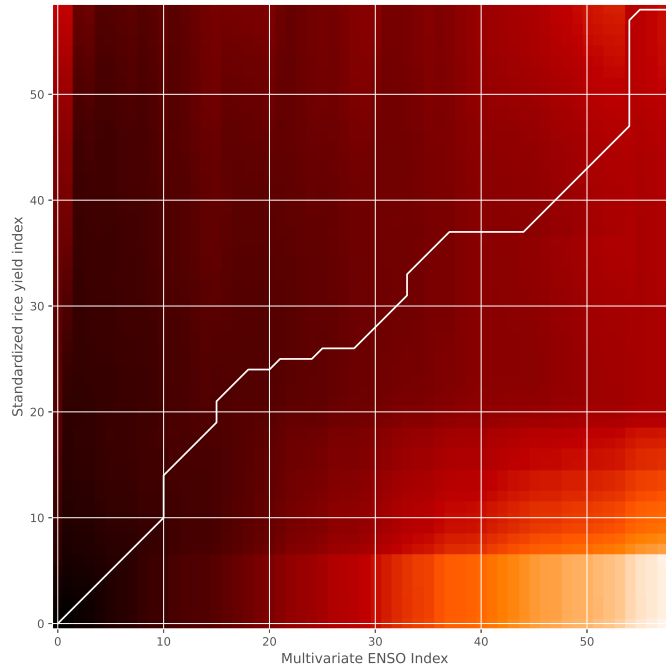


**Figure 2.** Lattice representation of cost matrix between ASRYI in Indonesia and annual average of MEI. The minimum path is shown in the white convex line.

82 With the minimum DTW path with minimum distance of 54.87, it can be concluded that the synchro-  
 83 nization process between the two time series is not efficient in terms of computational costs. However,  
 84 we cannot conclude whether there is no statistical relationship between the ENSO and rice production in

85 Indonesia. For this reason, we explore causal relationship between these two signals using the Wavelet  
 86 Coherence (WTC) algorithm.

87 The wavelet transform algorithm is intended to localize the change in time ( $\Delta t$ ) and angular frequency  
 88 ( $\Delta \omega$ ) of the time-series data into a function of frequency with respect to time, so that we can know  
 89 changes in time and frequency simultaneously (Torrence and Compo, 1998). One of the wavelet functions  
 90 that is often used in the fields of climatology is the Morlet transform, known as the continuous wavelet  
 91 transform (CWT), with the following equation,

$$\psi(\eta) = \pi^{-\frac{1}{4}} e^{i\omega_0} e^{-\frac{\eta}{2}} \quad (5)$$

92 , where  $\pi^{-\frac{1}{4}}$  is the normalized term and  $\eta = \frac{n}{s}$  is the dimensionless temporal parameter which is the  
 93 ratio of  $n$  as a time parameter and  $s$  as a scale parameter. The angular frequency parameter  $\omega_0$  is defined  
 94 as  $\omega_0 = \omega s$ . In the Morlet transform, the period of oscillation is  $P = 1.03s$ . CWT for a time-series  $x$  is  
 95 formally defined in the equation (6) as follows,

$$W_n(s) = \sum_{n'=0}^{N-1} x'_n \psi^* \left( \frac{(n' - n)\delta t}{s} \right) \quad (6)$$

96 In order to determine the relationship between the two time series, in the context of this study between  
 97 ASRYI and annual average of MEI, a complex conjugate multiplication these two CWT is needed as  
 98 shown in equation (7),

$$W_n^{xy}(s) = W_n^x(s) W_n^{y*}(s) \quad (7)$$

99 Phase coherence  $R_n(s)^2$  in WTC is obtained by normalizing and filtering the power spectrum  $|W_n^{xy}(s)|$   
 100 on the scale and time. Time smoothing is performed by normalizing using a Gaussian profile, while scale  
 101 smoothing is performed using a boxcar filter (Bloomfield et al., 2004). These two operations are indicated  
 102 by the  $\langle \dots \rangle$  expression in the following equation,

$$R_n^2(s) = \frac{|\langle s^{-1} W_n^{xy}(s) \rangle|^2}{\langle s^{-1} |W_n^x(s)|^2 \rangle \langle s^{-1} |W_n^y(s)|^2 \rangle} \quad (8)$$

103 To calculate the phase difference between these two time series, we use the comparison of the  
 104 imaginary term and the real term of  $W_n^{xy}$  as follows,

$$\phi(s) = \arctan \left( \frac{\Im \{ \langle s^{-1} W_n^{xy}(s) \rangle \}}{\Re \{ \langle s^{-1} W_n^{xy}(s) \rangle \}} \right) \quad (9)$$

105 We use the **biwavelet** package (Gouhier et al., 2021) in the R computing environment to automate  
 106 the WTC calculation process. This package is an implementation of the algorithm used by Grinsted et al.  
 107 (2004). This 2D representation of the WTC is shown in Figure 3. Time is displayed on the horizontal  
 108 axis, while the vertical axis shows the frequency (the lower the frequency, the higher the scale). Regions  
 109 in time-frequency space where the two time series co-vary are located by the WTC. Warmer colors  
 110 represent regions with significant interrelation, while colder colors signify lower dependence between the  
 111 sequences. Cold regions beyond the significant areas represent time and frequencies with no dependence  
 112 in the series. Arrows in this figure represents the lead/lag-phase relationship between annual average of  
 113 MEI and ASRYI. A zero phase difference means that the two sequences move together on a particular  
 114 scale. Arrows point to the right when the time series are in phase, yet if the arrows are pointing to the  
 115 right then both time sequences are in anti-phase. When this two-series data are in phase, it indicates that  
 116 they move in the same direction, and anti-phase means that they move in the opposite direction. Arrows  
 117 pointing to the right-down or left-up indicate that annual average of MEI is leading, while arrows pointing

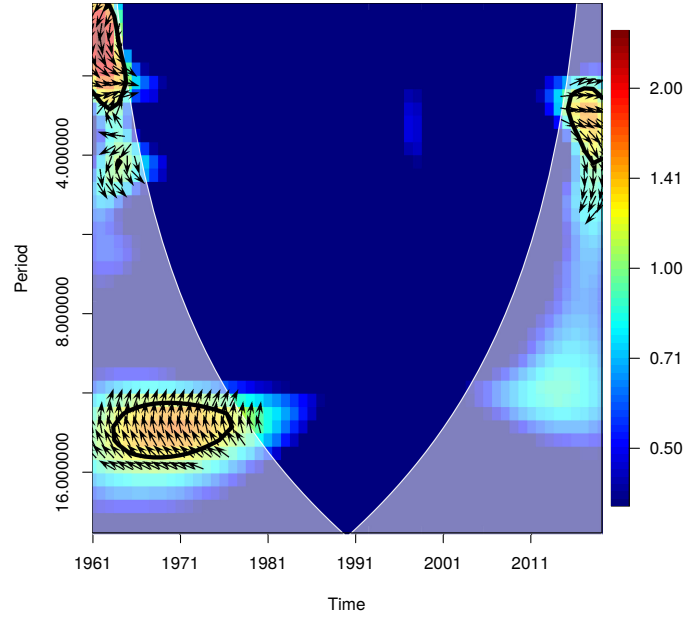


**Figure 3.** WTC between MEI and the rice yield index.

118 to the right-up or left-down show that the ASRYI is leading. In Figure 3, we do not see any significant  
 119 driving pattern of annual average of MEI on ASRYI, which belongs to the 95% cone of influence (COI)  
 120 determined by two degrees of freedom in the  $\chi^2$  distribution.

121 Based on the results we get from the DTW and WTC algorithms, we do not find a causal relationship  
 122 between the annual average of MEI and the ASRYI in Indonesia. However, to further ensure that there is  
 123 no statistical significance between these two variables, we try to make MEI as a covariate component  
 124 of the ASRYI sequence in the univariate Bayesian structural time-series (BSTS) framework (Scott and  
 125 Varian, 2014). We model the ASRYI  $y_t$  into a local linear trend with seasonality and regression (LLTSR)  
 126 model as follows,

$$y_t = \mu_t + \tau_t + \beta^T x_t + \varepsilon_t, \quad \varepsilon_t \sim \mathcal{N}(0, \sigma_\varepsilon^2) \quad (10)$$

127 , where  $\mu_t$  is a local linear trend,  $\tau_t$  is a seasonal component which is defined in equation (11) as  
 128 follows,

$$\tau_t = - \sum_{s=1}^{S-1} \tau_{t-s} + \omega_t, \quad \omega_t \sim \mathcal{N}(0, \sigma_\omega^2) \quad (11)$$

129 According to the total data points, the number of seasons  $S$  that we use in this model is 59. We  
 130 use a single vector covariate, the annual average of MEI  $x_t$  as the spike in the slab-spike priors, or in  
 131 other words we have the assumption that this variable will have a significant effect on ASRYI. The  
 132 regression coefficient  $\beta$  is calculated numerically. In this model, we also assume that the residual terms  
 133  $\omega_t$  and  $\varepsilon_t$  follow Gaussian distribution. We obtained the posterior density distribution of ASRYI by  
 134 using the Kalman filter, Kalman smoother, and 1000 times Markov Chain Monte Carlo (MCMC) process  
 135 automatically by utilizing the **bsts** package (Scott, 2020) in the R computing environment. Based on the  
 136 posterior density distribution of the non-residual components of the LLTSR model (Figure 4), we can see  
 137 that the prior regression component that we expect to have an effect, namely the annual average of MEI,  
 138 actually barely contributes to the ASRYI predictability. This is also further confirmed by the negative  
 139 inclusion probability value of the  $\beta$  regression coefficient which does not reach 20% (Figure 5).

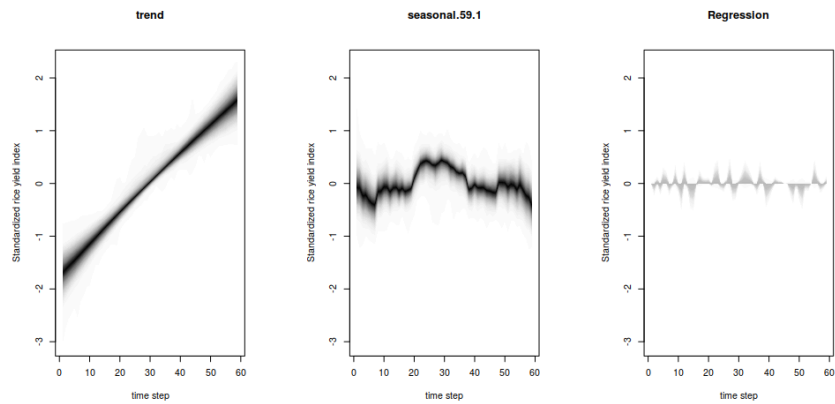


**Figure 4.** Posterior density distribution of local linear trend  $\mu_t$  (left), seasonal component  $\tau_t$  (center), and annual average of MEI  $\beta^T x_t$  as a regression component (right).

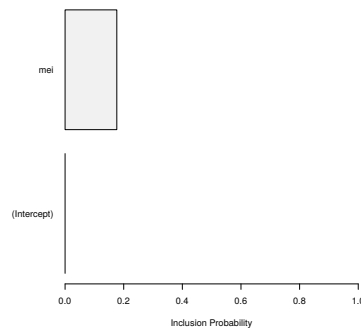


**Figure 5.** Covariate significance of the annual average of MEI. Grey bar here represents negative regression coefficient  $\beta$ .

### 140 3 DISCUSSION

141 As the results of those three methods, we do not find any association between MEI and yearly rice  
 142 production. We believe the results are caused by a few reasons. First one, the uncorrelated event may be  
 143 the consequence of having yearly periodicity for rice production rather than few months in a year. Also,  
 144 using a whole of Indonesian data rather than only specific region, may also arise problems. Of course, a  
 145 more detailed interannual time series analysis is also needed to solve this problem.

### 146 CODE AND DATA AVAILABILITY

147 Data are available through the cited sources throughout the article. Python and R scripts used in this study  
 148 are accesible at <https://github.com/sandyherho/ensoIndoRice>.

### 149 COMPETING INTEREST

150 The authors declare that they have no conflict of interest.

## 151 **AUTHOR CONTRIBUTION**

152 All authors designed the overall study. All authors contributed to the interpretation of the results and  
153 writing of the paper.

## 154 **ACKNOWLEDGEMENTS**

155 Cristy Q. Ho (PSU), Gisma A. Firdaus (P3GI), and Faiz R. Fajary (ITB) are acknowledged for stimulating  
156 insights and discussions. This study has been supported by Herho Group Corp., Rialto, CA, Knobz Store  
157 Bandung, and P3MI ITB.

## 158 **REFERENCES**

- 159 Berndt, D. J. and Clifford, J. (1994). Using dynamic time warping to find patterns in time series.  
160 In *Proceedings of the 3rd International Conference on Knowledge Discovery and Data Mining*,  
161 AAAIWS'94, page 359–370. AAAI Press.
- 162 Bloomfield, D. S., McAteer, R. T. J., Lites, B. W., Judge, P. G., Mathioudakis, M., and Keenan, F. P. (2004).  
163 Wavelet phase coherence analysis: Application to a quiet-sun magnetic element. *The Astrophysical*  
164 *Journal*, 617(1):623–632.
- 165 Deng, X., Huang, J., Qiao, F., Naylor, R. L., Falcon, W. P., Burke, M., Rozelle, S., and Battisti, D. (2010).  
166 Impacts of el niño-southern oscillation events on china's rice production. *Journal of Geographical*  
167 *Science*, 20(1):3–16.
- 168 FAO (1997). Food and Agriculture Organization of the United Nations. FAOSTAT Statistical Database.  
169 [Online; accessed 5. Jul. 2021].
- 170 Giorgino, T. (2009). Computing and visualizing dynamic time warping alignments in r: The dtw package.  
171 *Journal of Statistical Software*, 31(7):1–24.
- 172 Gouhier, T. C., Grinsted, A., and Simko, V. (2021). *R package biwavelet: Conduct Univariate and*  
173 *Bivariate Wavelet Analyses*. (Version 0.20.21).
- 174 Grinsted, A., Moore, J. C., and Jevrejeva, S. (2004). Application of the cross wavelet transform and  
175 wavelet coherence to geophysical time series. *Nonlinear Processes in Geophysics*, 11(5/6):561–566.
- 176 Ismail, N. W. and Chan, S. M. (2019). Impacts of the el niño-southern oscillation (enso) on paddy  
177 production in southeast asia. *Climate and Development*.
- 178 Naylor, R. L., Falcon, W. P., Rochberg, D., and Wada, N. (2001). Using el niño/southern oscillation  
179 climate data to predict rice production in indonesia. *Climatic Change*, 50:255–265.
- 180 Nguyen, N. V. (2005). Global climate changes and rice food security. [Online; accessed 14. Jul. 2021].
- 181 Panuju, D. R., Mizuno, K., and Trisasongko, B. H. (2013). The dynamics of rice production in indonesia  
182 1961–2009. *Journal of the Saudi Society of Agricultural Sciences*, 12(1):27–37.
- 183 Roberts, M. G., Dawe, D., Falcon, W. P., and Naylor, R. L. (2009). El niño–southern oscillation impacts  
184 on rice production in luzon, the philippines. *Journal of Applied Meteorology AND Climatology*,  
185 48:1718–1723.
- 186 Sakoe, H. and Chiba, S. (1978). Dynamic programming algorithm optimization for spoken word  
187 recognition. *IEEE Transactions on Acoustics, Speech, and Signal Processing*, 26(1):43–49.
- 188 Salvador, S. and Chan, P. (2004). Toward accurate dynamic time warping in linear time and space.  
189 *Intelligent Data Analysis*, 11:70–80.
- 190 Scott, S. and Varian, H. (2014). Predicting the present with bayesian structural time series. *International*  
191 *Journal of Mathematical Modelling and Numerical Optimisation*, 5:4 – 23.
- 192 Scott, S. L. (2020). *bsts: Bayesian Structural Time Series*. R package version 0.9.5.
- 193 Torrence, C. and Compo, G. P. (1998). A practical guide to wavelet analysis. *Bulletin of the American*  
194 *Meteorological Society*, 79(1):61–78.
- 195 Wolter, K. and Timlin, M. S. (1998). Measuring the strength of enso events: How does 1997/98 rank?  
196 *Weather*, 53(9):315–324.
- 197 Wright, S. (2020). Largest Rice-Producing Countries. *WorldAtlas*.